

A key to the spectral variability of prompt GRBs

Mikhail V. Medvedev

Department of Physics and Astronomy, University of Kansas, Lawrence, KS 66045

Abstract. We demonstrate that the rapid spectral variability of prompt GRBs is an inherent property of radiation emitted from shock-generated, highly anisotropic small-scale magnetic fields. We interpret the hard-to-soft evolution and the correlation of the soft index α with the photon flux observed in GRBs as a combined effect of temporal variation of the shock viewing angle and relativistic aberration of an individual thin, instantaneously illuminated shell. The model predicts that about a quarter of time-resolved spectra should have hard spectra, violating the synchrotron $\alpha = -2/3$ limit. The model also naturally explains why the peak of the distribution of α is at $\alpha \sim -1$. The presence of a low-energy break in the jitter spectrum at oblique angles also explains the appearance of a soft X-ray component in some GRBs and their paucity. We emphasize that our theory is based solely on the first principles and contains no ad hoc (phenomenological) assumptions.

INTRODUCTION

Rapid spectral variability is a remarkable, yet unexplained feature of the prompt GRB emission. The variation of the hardness of the spectrum and the hard-to-soft evolution are the most acknowledged features [1, 2, 3]. A quite remarkable “tracking” behavior, when the low-energy spectral index α follows (or correlates with) the photon flux [2] is particularly intriguing. An example of such a trend is shown in Fig. 1 (we used data from [4]).

THEORY OF JITTER RADIATION

The angle-averaged spectral power emitted by a relativistic particle moving through small-scale Weibel-generated magnetic fields is given here without derivation (see [5, 6] for details):

$$\frac{dW}{d\omega} = \frac{e^2 \omega}{2\pi c^3} \int_{\omega/2\gamma^2}^{\infty} \frac{|\mathbf{w}_{\omega'}|^2}{\omega'^2} \left(1 - \frac{\omega}{\omega' \gamma^2} + \frac{\omega^2}{2\omega'^2 \gamma^4} \right) d\omega'. \quad (1)$$

Here γ is the Lorentz factor of a radiating particle and $\mathbf{w}_{\omega'} = \int \mathbf{w} e^{i\omega' t} dt$ is the Fourier component of the transverse particle’s acceleration due to the Lorentz force. This temporal Fourier transform is taken along the particle trajectory, $\mathbf{r} = \mathbf{r}_0 + \mathbf{v}t$.

Because the Weibel-generated magnetic fields at a shock are highly anisotropic, as shown in Figure 2, the spectra of radiation emitted by an electron in such fields depend on the viewing angle Θ between the normal to the shock and the particle velocity in the

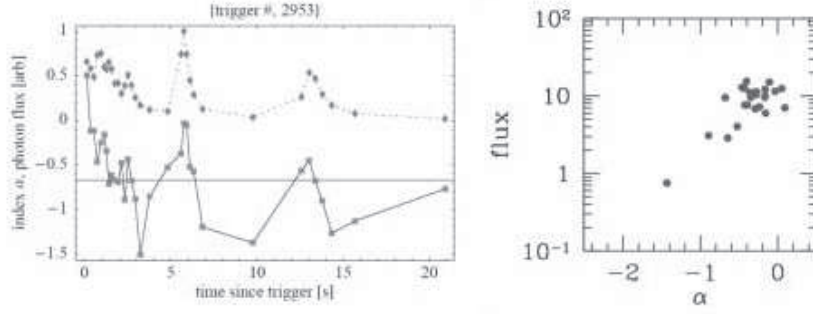


FIGURE 1. (a) — A tracking GRB: normalized flux (diamonds) and the soft spectral index α (squares) evolve similarly with time. (b) — Scatter plot of flux vs. α for GRB940429.

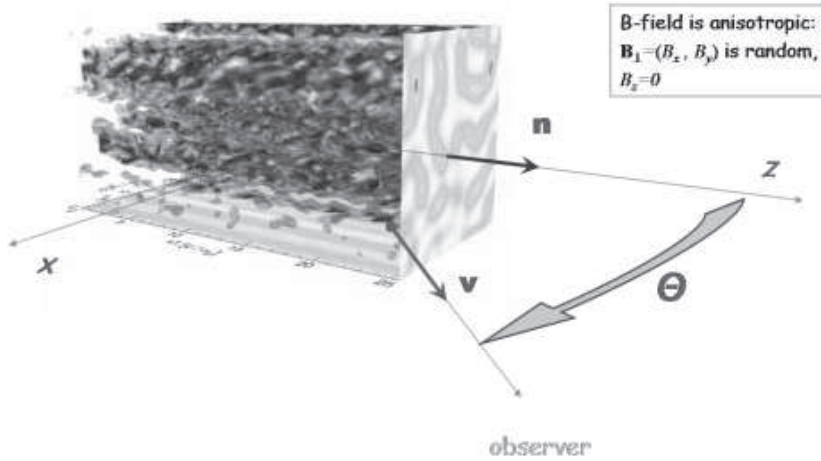


FIGURE 2. Magnetic filaments in a shock [7]. The radiation spectrum varies with the viewing angle Θ .

shock co-moving frame, which is approximately the direction toward an observer, for an ultra-relativistic particle. The acceleration spectrum is

$$\langle |\mathbf{w}_{\omega'}|^2 \rangle = C/2\pi (1 + \cos^2 \Theta) \int f_z(k_{\parallel}) f_{xy}(k_{\perp}) \delta(\omega' + \mathbf{k} \cdot \mathbf{v}) dk_{\parallel} d^2 k_{\perp}, \quad (2)$$

where C is the normalization of the magnetic field spectrum over spatial scales to the total field energy density $B^2/8\pi$. Here f_{xy} and f_z determine spectra of the magnetic fields in the shock plane and in the direction of the shock motion. These spectra are independent of each other to a large degree, as indicated by numerical simulation (e.g., [8]). We assume f_{xy} and f_z are broken double-power-laws,

$$f_z(k_{\parallel}) = k_{\parallel}^{2\alpha_1} / (\kappa_{\parallel}^2 + k_{\parallel}^2)^{\beta_1}, \quad f_{xy}(k_{\perp}) = k_{\perp}^{2\alpha_2} / (\kappa_{\perp}^2 + k_{\perp}^2)^{\beta_2}, \quad (3)$$

with the position of the break (peak) determined by the Weibel scale: the plasma skin depth, $\kappa_{\perp} \sim \kappa_{\parallel} \sim \omega_p/c$.

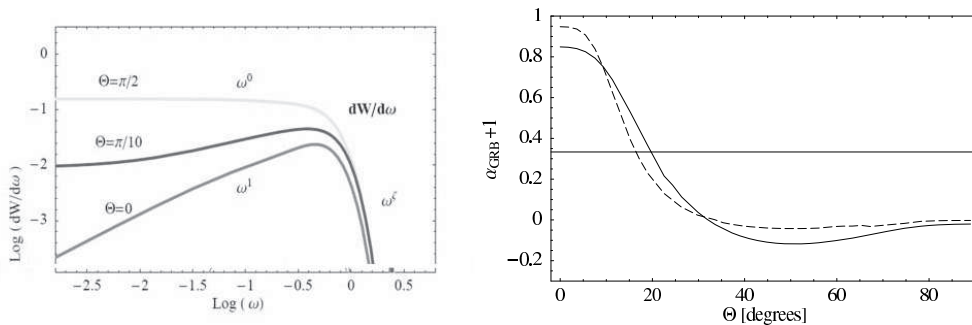


FIGURE 3. (a) — Typical spectra for three viewing angles, $\Theta = 0, \pi/10, \pi/2$. (b) — Soft spectral index as a function of Θ at energies 10 (solid) and 30 (dashed) times below E_p .

INTERPRETATION OF PROMPT GRB SPECTRA

The typical jitter radiation spectra for three different angles are shown in Figure 3a. When a shock velocity is along the line of sight, the low-energy spectrum is hard $F_\nu \propto \nu^1$, harder than the “synchrotron line of death” ($F_\nu \propto \nu^{1/3}$). As the viewing angle increases, the spectrum softens, and when the shock velocity is orthogonal to the line of sight, it becomes $F_\nu \propto \nu^0$. Another interesting feature is that at oblique angles, the spectrum does not soften simultaneously at all frequencies. Instead, there appears a smooth spectral break, which position depends on Θ . The spectrum approaches $\sim \nu^0$ below the break and is harder above it. This softening of the spectrum at low ν 's could be interpreted as the appearance of an additional soft X-ray component, similar to that found in some of GRBs [9].

Figure 3b shown the low-energy slope at a frequency 10 and 30 times lower than the spectral peak. These frequencies correspond to the edge of the *BATSE* window for bursts with the peak energy of about 200 keV and 600 keV, respectively. Hence, the spectral slope, α_{GRB} , will be close to those obtained from the data fits. Since $\Theta(t)$ increases with time during an individual emission episode, the curves roughly represent the temporal evolution of α_{GRB} . Assuming that time-resolved spectra are homogeneously distributed over Θ , one can estimate the relative fraction of the synchrotron-violating GRBs (i.e., those with $\alpha_{\text{GRB}} + 1 > 1/3$) as about 25%, which is very close to the 30% obtained from the data [4]. Most of the GRBs, $\sim 75\%$, should, by the same token, be distributed around $\alpha_{\text{GRB}} \sim -1$. Note also that time-integrated GRB spectra should have α_{GRB} around minus one, as well.

In the standard internal shock model, each emission episode is associated with illumination of a thin shell, — an internal shock and the hot and magnetized post-shock material. We assume that the shell is spherical (at least within a cone of opening angle of $\sim 1/\Gamma$ around the line of sight) and this shell is simultaneously illuminated for a short period of time. The observed photon pulse is broadened because the photons emitted from the patches of the shell located at larger angles, ϑ , from the line of sight arrive at progressively later times. The bolometric flux depends on ϑ , and hence on time as [3]:

$$F_{\text{bol}} = F_0 \mathcal{D}^2(\Theta) / \Gamma^2 \quad (4)$$

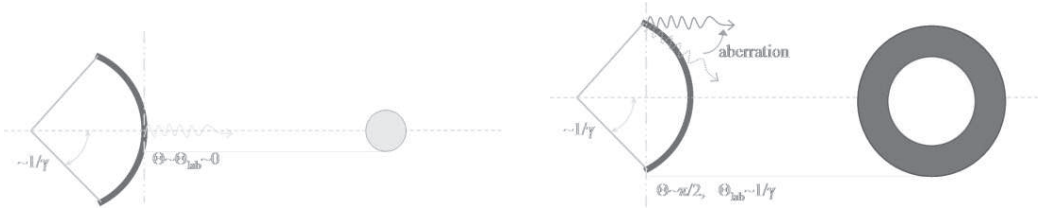


FIGURE 4. Cartoon explaining correlation of the spectral index and the flux as a combined effect of the anisotropy of jitter radiation and relativistic aberration.

with the Lorentz boost

$$\mathcal{D}(\Theta) = [\Gamma(1 - \beta \cos \vartheta)]^{-1} = \Gamma(1 + \beta \cos \Theta) = [\Gamma(1 - \beta - \beta c\Delta t/R_0)]^{-1}. \quad (5)$$

Because of relativistic aberration, the comoving viewing angle, Θ , is greater than ϑ and approaches $\Theta \sim \pi/2$ (the shell is seen edge-on) when $\vartheta \sim 1/\Gamma$. Thus, there must be a tight correlation between the observed spectrum and the observed photon flux, because they are, in essence, different manifestations of the same relativistic kinematics effect. An observer first detects photons emitted close to the line of sight, for which $\vartheta \sim \Theta \sim 0$, see Figure 4a. The flux is the largest and α is the hardest (around 0) at this time. As time goes on, an observer sees photons emitted farther from the line of sight, as in Figure 4b. The flux decreases, whereas α becomes softer and approaches -1 . Of course, we neglected cooling effects here, which can result in even softer spectra with $\alpha \sim -3/2$.

ACKNOWLEDGMENTS

This work has been supported by NASA grant NNG-04GM41G, DoE grant DE-FG02-04ER54790, and the KU GRF fund.

REFERENCES

1. P.N. Bhat, et al., *Astrophys. J.* **426**, 604 (1994).
2. A. Crider, et al., *Astrophys. J. Lett.* **479**, L39 (1997).
3. F. Ryde, and V. Petrosian, *Astrophys. J.* **578**, 290 (2002).
4. R.D. Preece, M.S. Briggs, R.S. Mallozzi, G.N. Pendleton, W.S. Paciesas, D.L. Band, *Astrophys. J. Suppl.* **126**, 19 (2000).
5. M.V. Medvedev, *Astrophys. J.* **540**, 704 (2000).
6. M.V. Medvedev, astro-ph/0510472, *Astrophys. J.* in press (2006).
7. M.V. Medvedev, L.O. Silva, M. Kamionkowski, astro-ph/0512709 (2005).
8. J.T. Frederiksen, C.B. Hededal, T. Haugbølle and Å. Nordlund, *Astrophys. J. Lett.* **608**, L13 (2004).
9. R.D. Preece, et al., *Astrophys. & Space Sci.*, **231**, 207 (1995).